Evidence for 21-Helicity of Poly[9,9-bis(2-ethylhexyl)fluorene-2,7-diyl]

Matti Knaapila,[†,§] Mika Torkkeli,*[,‡] and Andrew P. Monkman[§]

MAX-lab, Lund University, POB 118, SE-22100 Lund, Sweden; Department of Physical Sciences, POB 64, FI-00014, University of Helsinki, Helsinki, Finland; and Department of Physics, University of Durham, South Road, Durham DH1 3LE, UK

Received November 20, 2006; Revised Manuscript Received March 8, 2007

ABSTRACT: The conformational state of the π-conjugated polyfluorene poly[9,9-bis(2-ethylhexyl)fluorene-2,7-diyl] is reconsidered. Contrary to the general opinion, this helical polymer is shown to organize in a giant repeat consisting of 21 monomer units. The length of the unit cell of 16.97 nm is suggested.

Introduction

Helical polymers represent one of the very few architectures where structural units can extend over very long (tens of nanometers) meridional distances. Although helicity is common among crystalline polymers,[1] they typically involve fairly simple chain architectures, where the unit cells are a few nanometers at most,[2] while exotic long repeat/high turn helices are more often encountered in the realm of filamentous plant viruses[3] or superstructures found, e.g., in helicenes.[4]

Rigid π-conjugated backbone may in principle incite to meridionally larger repeat units, but despite their rich structural variations[5] in higher helical π-conjugated polymers, they have remained a largely unexplored field. Functional synthetic polymers in general[6] may have potential applications related to helicity, such as nanopattern formation on surfaces.[7]

Perhaps the most archetypical π-conjugated polymer, poly-[9,9-bis(2-ethylhexyl)fluorene-2,7-diyl] (or PF2/6, see inset in Figure 1) with excellent stability and optoelectronic properties,[8] provides an ideal case. Since the first structural studies by Lieser et al.,[9] the conformational properties of this particular polyfluorene have been the subject of vast theoretical and experimental investigations.[10] The helical form was determined as either 5_1 or 5_2 and has not been challenged in later diffraction experiments of the polymer[11,12] or its oligomers.[13] Both quantum chemical calculations[9,11] and simulations[12,14] select 5_2 as the more likely alternative.

However, the experimental evidence of 5-fold periodicity is based on just two meridional layer lines in the X-ray diffraction (XRD) and electron diffraction (ED) patterns of oriented fibers[9] and thin films.[11] These correspond to periodicities 0.808 nm and ca. 4 nm along the polymer axis. The first value is determined with good accuracy from a strong reflection along the fiber axis, and it most naturally corresponds to the monomer repeat. The second value is less well-defined since the most prominent reflection on this layer line is very close to the first (equatorial) hexagonal peak. Thus, when the sample is not well oriented, its axial position is not very precisely determined. It is certainly precise enough to exclude the 6-fold helical form. However, in our investigations of aligned thin films of PF2/6, we have noted a systematic deviation from the 1:5 ratio in these periodicities.[11] Apart from the mentioned ED work,[9] these represent the best achieved orientation in PF2/6. We have also noticed tiny reflections along the meridional, which do not quite

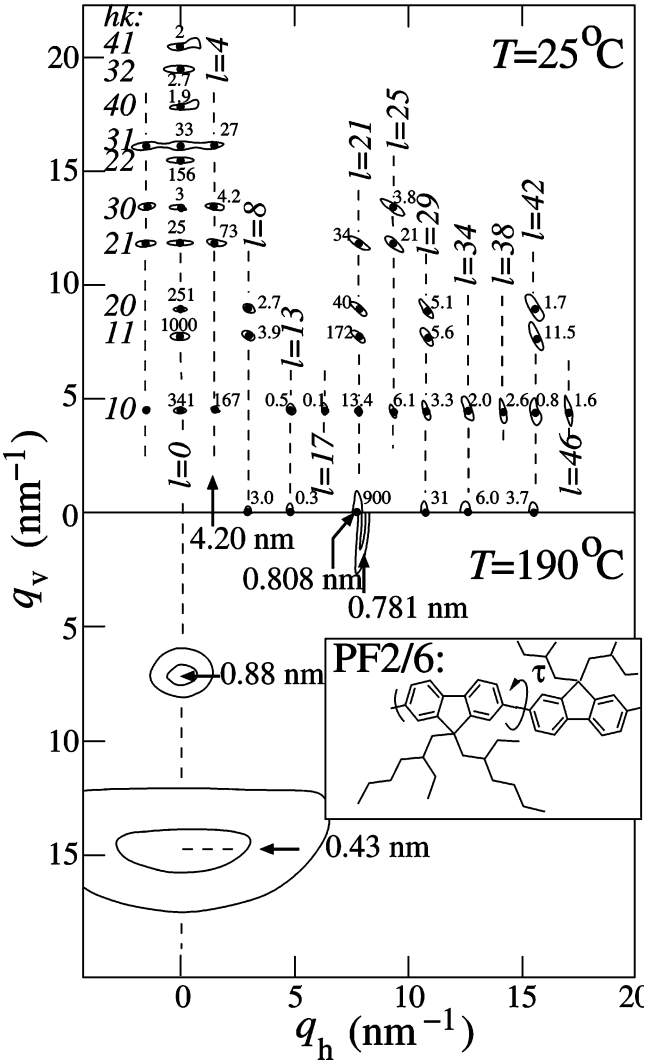

Figure 1. Observed X-ray fiber diffraction maxima from PF2/6 (M_n = 29 kg/mol, M_w = 68 kg/mol) at room temperature (upper panel) and at 190 °C (lower panel). The inset shows the chemical structure of the polymer and its orientation with respect to the diffraction patterns. Relative intensity values are marked beside each reflection. q_v and q_h denote components of the q vector ($q = 4\pi \sin\theta/\lambda$, where θ is half the scattering angle and λ the wavelength) along the equatorial and meridional (chain axis) directions. The layer lines at the various q_h values are drawn based on the new proposed 21-helicity.

* Corresponding author. E-mail: mika.torkkeli@helsinki.fi.
† Lund University.
‡ University of Helsinki.
§ University of Durham.

10.1021/ma0626665 CCC: $37.00
Published on Web 04/24/2007

Table 1. Observed Relative Peak Positions q_h along the Meridional and along the First Four Hexagonal Orders *hk*

hexagonal order *hk*					expected at	
00	10	11	20	21	5-helix	21-helix
	0.191			0.191	0.2000	0.1905
0.383		0.383	0.380		0.4000	0.3810
0.618	0.622				0.6000	0.6190
1[a]	1	1	1	1	1.0000	1.0000
	1.193			1.191	1.2000	1.1905
1.381	1.382	1.384	1.383		1.4000	1.3810
1.622	1.617				1.6000	1.6190
	1.810				1.8000	1.8095
1.995	1.997	2.001	1.995		2.0000	2.0000

[a] Values are normalized to this layer line.

fit the proposed 5-monomer periodicity.[15] In this paper we consider these "anomalous'' reflections as part of the crystalline structure which we reevaluate accordingly.

An intriguing open question concerns the interchain packing of polyfluorenes (PFs) and its relation to the helical state. The unit cell of PF2/6 is either hexagonal or marginally monoclinic,[12] with three chains per unit cell.[9] It has been difficult to understand why the 5-fold helix should adopt a threewise packing in seemingly good hexagonal order. Instead, one would expect a low-symmetry triclinic crystal, pseudohexagonal packing of single chains, or tetragonal symmetry containing equal amounts of enantiomers.[1] The current view, where we have a two hierarchical levels of noncrystallographic symmetry leading to 3-D crystalline arrangement, is therefore not satisfactory.

We have now recorded fiber X-ray diffraction patterns of exceedingly well-aligned samples to better address the question of crystalline form.

Experimental Section

Sample Preparation. The synthesis of PF2/6 has been described elsewhere.[8] To prepare well-oriented samples, PF2/6 (molecular weight $M_n = 29$ kg/mol, $M_w = 68$ kg/mol) was sheared in the melt state on a smooth surface and allowed to cool slowly to room temperature. We estimate that the axial orientation is comparable to thin films on alignment substrates but without the surface-induced orientation of hexagons, and thus the samples may be considered to have a fiber texture. The axial orientation is sufficiently wide to give layer lines up to diffraction angle 10° without rocking the sample.

X-ray Diffraction. The measurements were conducted at the Beamline W1.1. at the Hamburger Synchrotronstrahlungslabor of the Deutsches Electronen Synchrotron (DESY). The beam was monochromatized with a double-crystal Si(111) monochromator, and X-ray energy 10.5 keV was used. The beam was reduced with slits to 0.2 × 1 mm, and the diffraction pattern was recorded with a flat image plate at 355 mm distance.

Results and Discussion

Crystal Structure. Figure 1 shows a typical pattern in contour representation in the crystalline (25 °C) and nematic (190 °C) states. The hexagonal reflections $q_a\sqrt{n}$, where $n = h^2 + k^2 + hk$ are found along the layer line $l = 0$ (vertical in the figure). Note that 300 is barely visible, and 210 is 3 times weaker than the residing off-equatorial peaks. We can distinguish about 20 off-equatorial reflections. Mostly, these occur at the first four hexagonal orders because reflections tend to fan out due to axial spread of the polymers and paracrystalline nature of hexagonal packing.

The determined axial positions q_h of the reflections are collected in Table 1. They are significantly far removed from those expected for the 5-helix but correspond remarkably well to a unit cell, which is 21 times the monomer repeat, or $c = 16.97$ nm. We therefore put forward that PF2/6 is a 21-helix in the solid state. The layer line at $q_h = 7.78$ nm^{-1} still corresponds to the monomer repeat, but we now label it as $l = 21$ in Figure 1. The previous assignment of 5-fold helicity was based on the reflection 104.

We have also reexamined earlier published GIXD data and observed that the reflections, which were at the time labeled as "close to 002 and 007'',[16] are actually 008 and 00 29. Thus, 21-helicity is not restricted to just this sample. Unlike linear side-chain PFs, such as poly[9,9-dioctylfluorene-2,7-diyl] (PF8)[17,20] or poly[9,9-dihexylfluorene-2,7-diyl] (PF6),[21] only one crystalline morphology seems to exists for PF2/6.[12]

The strong reflections found at $l = 4$ and $l = 8$ are most likely associated with the helical pitch (P), either $P = 4.2$ nm (21_4 helix) or $P = 2.1$ nm (21_8 helix). These helices are structurally very close to 5_1 and 5_2; the torsional angles are smaller by 3.5° and 7°, respectively—in our molecular model 65° and 136°. The 21-helix has a 3-fold screw axis so it is immediately suited for hexagonal order. From packing considerations, however, it is even harder to accommodate in a hexagonal lattice because the nonsymmetric element now comprises seven monomers instead of five for the 5-helix. In view of these similarities, the new model does not really resolve the problem of interchain packing nor does it require any rethinking of diffraction data vis-á-vis molecular dynamic simulations, for example.

The Form of Helices. The more important question still remains whether the chain conformation is 21_4, which is a wide helix with side chains pointing inward, or 21_8, which is a practically linear rod with side chains pointing outward, resembling a bottle brush. Several simulations and calculations exist for PF2/6 and related polyfluorenes.[9,12,14] These in unison favor the trans-type conformer, where the torsion angle τ is about 140°. Crystalline studies of fluorene dimer[13] show $\tau = 144.2°$. Interestingly though, this form does not fit well into the diffraction data of the polymer. At least three arguments can be made to support 21_4 helical form over 21_8 (or likewise 5_1 helix over 5_2): (1) The monomer repeat $p = 0.808$ nm as observed from the most prominant meridional reflection is significantly shorter than in linear side chain PFs ($p \sim 0.830$ nm), where τ is close to 180°.[17,21.] (2) Observed intensities on the equatorial *hk0* plane, in particular the weak 210 and 300, are more compatible with the lateral dimensions of the 21_4 helix. (3) The strong intensities on the $l = 4$ and $l = 25$ layer lines support the view that these lines correspond exactly the helical pitch.

These are general guidelines rather than actual proofs since they are drawn from consideration of single-chain structure factors and, more importantly, do not correspond to space-filling conformations of side chains. The second argument in special should be dealt with caution. We shall nevertheless discuss the scattering in light of these arguments, justified by the long repeat of the main chain and the disordered state of the side chains which would render the single helix as approximately centrosymmetric when viewed along the polymer axis and resembling an ideal helix.

The monomer repeat of course depends on the molecular form. However, for $\tau \approx 140°$ the repeat would be only 2 pm smaller than for the all-trans chain. Otherwise, the observed difference in p requires a radically different backbone structure. The calculated monomer repeat for both 5_1 and 21_4 models agree almost perfectly with experiment. In the nematic state (Figure 1, lower panel), the fluorene repeat is shorter, so the torsion angle *decreases* on melting.

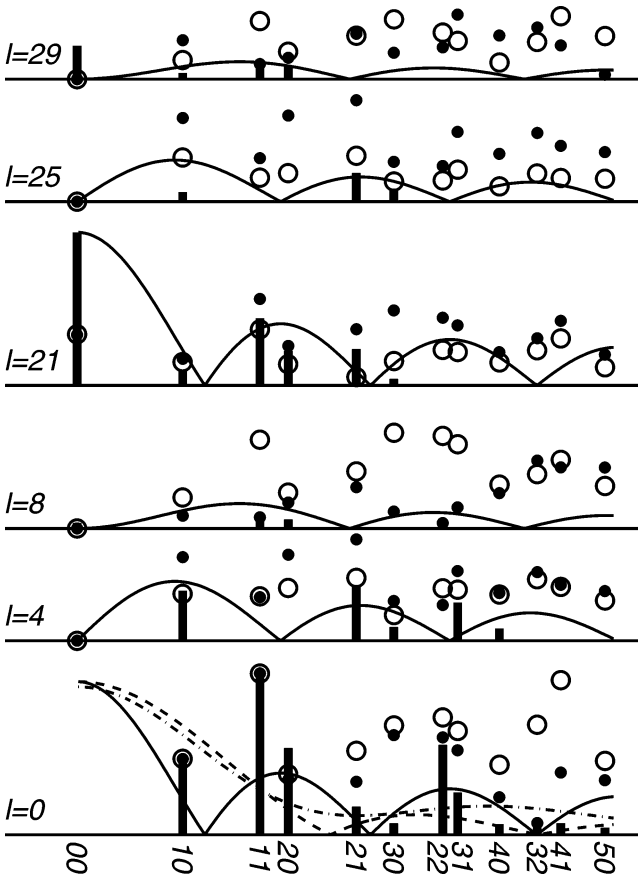

Figure 2. Comparison between *hkl* diffraction amplitudes for 21_4 (●) and 21_8 (○) helices. The vertical bars represent measured values. The solid curves at the $21n$, $21n + 4$, and $21n + 8$ lines are respectively the Bessel functions $J_0(qR)$, $J_1(qR)$, and $J_2(qR)$ with $R = 0.46$ nm, and the dashed and dash-dotted curves represent amplitudes calculated for single helices using the sum of Bessel functions formula.

To illustrate arguments (2) and (3), Figure 2 shows the diffraction amplitudes of 21_4 and 21_8 helices normalized to the strongest reflection 110. In both cases we have adopted similar trial conformation of the side chains, parallel to the backbone and refined their positions for best correspondence with the experimental data. The selected symmetry in Figure 2 is $P3_2$, which is left-hand rotation for the chosen right-hand helix, but $P3$ symmetry gives precisely the same results. For the left-hand helix compatible symmetries are $P3_2$ and $P3$.

On the equatorial ($l = 0$), the intensities of the first 2−3 peaks mostly reflect the positions of the three helices within the unit cell, being close to the special points where the interchain separations are the largest, while the helix form and the side chains affect higher orders. In light of the high cylinder symmetry, the structure factor for the single helix in the $l = 0$ plane can be written in terms of zeroth-order Bessel functions[22]

$$F(q) = \sum_j f_j J_0(qr_j) \tag{1}$$

where f_j are the atomic scattering factors and r_j the distance of the jth atom from the helical axis. With a proper choice of side-chain conformation, reflections 210 or 300 may be made to disappear for the 21_4 helix but not for the 21_8 helix which has a smaller backbone radius. The near extinctions may of course result from interchain interference effects, i.e., packing of three chains in the unit cell.

For the layer lines with $l \neq 0$ a structure factor formula similar to eq 1 applies, involving higher order Bessel functions.[22] Without going into details of analysis, the outcome corroborated by direct structure factor calculations is that we will get significant intensity only at the axial q positions

$$\frac{q}{2\pi} = \frac{n}{P} + \frac{m}{p} \tag{2}$$

where n and m are integers p is the monomer repeat and P is the helical pitch. For a 21_4 helix, we see reflections at layer lines $l = 21m \pm 4n$, while 21_8 would diffract on $l = 21m \pm 8n$. In fact, a strictly regular 21_8 helix will not produce *any* intensity on $l = 21m \pm 4n$. In Figure 2 we have purposely invoked the two-pitch periodicity into 21_8 by flipping the directions of the side chains on average every $21/8 = 2.62$ monomers. Still, the intensities on $l = 4$ tend to be weaker than on $l = 8$, contrary to experiment.

There are systematic absences of reflections on the various layer lines. The cited theory of Cochran, Crick, and Vand[22] predicts that the scattering amplitudes on the $l = 21n$, $l = 21n + 4$, and $l = 21n + 8$ are dominated by J_0, J_1, and J_2, respectively. Figure 2 aims to demonstrate that the variation of the diffracted amplitude along the layer lines is qualitatively explained by the form factor of a single uniform helix of radius 0.46 nm. This again ignores any interference effects between helices. These are however included in the calculation of the structure factor from the atomistic models (circles and bullets). Argument (3) is then twofold: The diffracted intensity on the fourth layer line in the case of 21_8 helix can only result from deviation from this helicity, e.g., side-chain disorder. The fact that the intensities are higher on the fourth layer than the eighth does not reconcile with this view. On the other hand, the variation of intensity on the layer lines resembles more the expected behavior for 21_4 helix. We stress that interference effects may obscure these effects: Indeed, the structure factor calculations only scantly follow the ideal uniform helix model.

The anomalous spots on the meridional 008 and 00 29 do not follow *directly* from helicity but are due to periodic disorder, which is induced by steric packing of the chains in a symmetry, which differs from the helix symmetry.[23] The observed period 2.1 nm ($P/2$) may indicate a zipper type contact with 21_4 helices.

Side-Chain Conformation.The peculiar structural properties of PF2/6 seem to stem from the introduction of ethyl branch in the side chain and they have been carefully studied.[12] The linear chain PF8 has a rich phase behavior and is able to form a truly crystalline phase with sharp diffraction peaks throughout.[17] The side chains are likewise crystalline and may also extend perpendicularly from the backbone.[18] In contrast, the side chains in PF2/6 are disordered, and this seems to apply even to the dimeric and monomeric forms.[13]

In PF8, three groups of conformer isomers, α, γ, and β, have been identified in which the torsion angles are 135°, 150°, and 160°, respectively.[19] The last of these realizes the agg sequence of side-chain torsion angles which causes side chains to orient parallel to the helical axis. In PF2/6, two groups of low-energy conformers emerge with main-chain torsion angle about 50° and 135° and one particularly low in energy at $\tau = 35°$.[12] In broad terms the behavior for all PFs follows the potential energy of difluorene, which shows two equal minima at 45° and 135°.[25] The conclusion is that side-chain conformation has a minor effect on an isolated chain whereas interchain interactions and side-chain packing are of more importance. Thus, both side-chain and main-chain local structure may be entirely different in bulk polymer compared to oligomers[13] or polymer solutions[24,26] and also between linear and branched side-chain PF's.

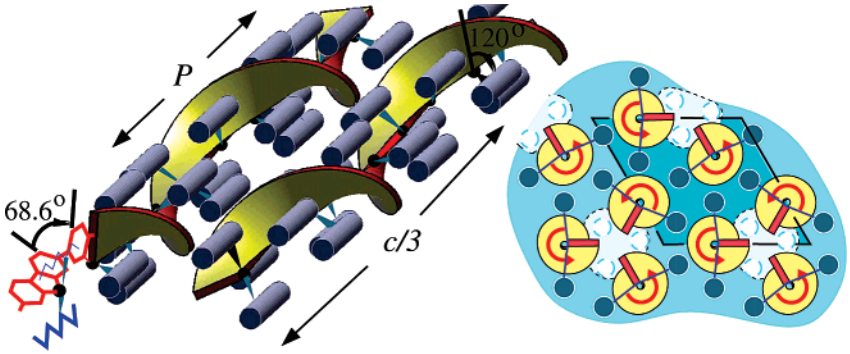

Figure 3. Schematic proposal for the helix form and side-chain packing. In the 21_4 helix, the link atom is at the helical axis, around which the main chain and the two side chains revolve quite like in a triple helix. The helical pitch *P* is defined by one complete turn of the backbone. The 21-helicity means that after one-third of the repeat distance *c* the helix has undergone a 120° rotation. The right drawing shows possible arrangement of the side chains. The dashed areas correspond to sites unoccupied in this particular monomer layer.

Using structure factor (SF) refinement, Tanto et al.[12] found a necessary perpendicular conformation for the side chains. This outcome is in practice dictated by the strength of the 0.8 nm peak (00 21). Calculations with parallel chain always yield much weaker reflection (cf. Figure 2), even when main chains are axially in full register. However, a significant part of intensity in this peak may be due to noncrystalline material (cf. Figure 1, bottom panel), so SF calculations may not give useful information on the side-chain conformations.

The thermotropic nematic state (see Figure 1 bottom) displays two maxima in the equatorial direction. The first corresponds to main-chain separation and the second a distance 0.43 nm. The latter peak is typical for aliphatic molecules, e.g., hexane, and suggests parallel orientation of the side chains. Thus, the nematic state is characterized by hexagonal packing of single chains and simultaneous parallel packing of the side chains. These also appear as strong diffuse spots underneath 110 and 220 in the crystalline state. The strong 220 reflection indicates side-chain packing with separation approximately half the interchain distance. This is shown schematically in Figure 3.

Possibly, the side chains are too bulky to conform into the 6-fold symmetry so a less dense crystallizable symmetry is chosen. From the site packing considerations alone 21_4 and 21_8 are identical. In 21_4, however, the side chains should be closer to the helical axis, and the whole package is more compact. Note that regardless of what form the helix takes, there is always a packing frustration in a sense that, of the six side-chain sites encompassing each monomer, two are occupied by its side chains and further two by its close neighbors. This leaves two vacant sites, a gap opposite to the link atom. Thus, there is little incentive for the chain to take the more natural 6-fold symmetry.

Helicity and Phase Behavior. Since the 21-helix has a 3-fold screw symmetry, we anticipate that the helix is periodic within the hexagonal crystal, and the repeat distance is thus 16.97 nm. This may have interesting implications in the phase behavior. Incidentally, the length corresponds to ca. 8 kDa molecular weight, which is only slightly smaller than the observed threshold molecular weight *M** for the onset of crystallinity in PF2/6[15] and could thus contribute to the observed phase behavior. In principle, the repetitive unit could be seven monomers *provided* that helices occupied the special position (1/3,0,0). This, however, is at odds with the occurrence of reflections 100, 200, etc. Thus, the organization of side chains is perhaps not commensurate with the main helix threefold symmetry and may vary between unit cells. The coherence length along *c*-axis as indicated by widths of 00l reflections is about 22 nm.[11,16] This is likely an underestimation due to inherent poor resolution in thin film diffraction. Then helical order seems to persist at least up to 1.5−2 unit cells (30−40 monomers, 6−8 helical turns). The same result is obtained for monomer periodicity and pitch periodicity.

Below *M**, PF2/6 forms a nematic phase, which is different from the thermotropic LC phase.[15] This phase shows a broad remnant of the 100 reflection, indicating that the three-helix motif is there but without long-range order. Similar nematic is also obtained by rapid cooling from the melt state, and Chi et al.[13] have even reported this phase in monodisperse 4-mers to 7-mers. Thus, the formation of the trimer of helices seems to be a separate issue from their crystallization. The transition from thermotropic nematic to crystalline on cooling is sluggish and requires lengthy annealing process, and the material shows considerable hysteresis on thermal cycling. These phenomena may result from the implied two-step crystallization process, one involving formation of regular helices for more efficient steric packing and the other for their organization into a regular symmetric structure. Judging from the similarities in the diffraction data, the changes in backbone conformation are small. In the (lyotropic) nematic state the monomer period is 0.78 nm, from which an average torsion angle 50° can be calculated. This agrees well with the minimum conformation states of single helices.[12]

Conclusions

In conclusion, the results presented here show that the periodicity of PF2/6 is 21 times the monomer repeat instead of 5 times as was thought before. We suggest therefore that it crystallizes in a 21-helical form. We should stress that the structure is not perfectly crystalline due to side-chain disorder and resulting hexagonal paracrystallinity.[15] Diffraction data also show a presence of 21_4 helical motif within the crystal. This does not necessarily mean that the *backbone* of the polymer has this helical form, which could also be realized even through some concerted arrangement of 21_8 helices in close hexagonal packing. However, the unforced way in which the 21_4 backbone qualitatively describes the diffraction data makes it in our opinion a more likely alternative. It seems that, before refining the presented model further, the symmetry aspects need to be reconsidered and perhaps more complex helical forms[27] should also be screened.

Acknowledgment. This study has been funded by One North-East UIC Nanotechnology Grant. M.T. and M.K. acknowledge support from DESY (Contract RII3-CT-2004-506008 (IA-SFS)). We are also indebted to Prof. U. Scherf of the University of Wuppertal for providing us with PF2/6 as well as W. Caliebe and O. H. Seeck of DESY for technical assistance.

References and Notes

(1) Tadokoro, H. *Structure of Crystalline Polymers*; John Wiley & Sons: New York, 1979.
(2) Vogl, O.; Jaycox, G. D. *Polymer* **1987**, *28*, 2179.
(3) Stubbs, G. *Rep. Prog. Phys.* **2001**, *64*, 1389.
(4) Eskildsen, J.; Krebs, F. C.; Faldt, A.; Sommer-Larssen, P.; Bechgaard, K. *J. Org. Chem.* **2001**, *66*, 200.
(5) Winokur, M. J. In *Handbook of Conducting Polymers*; Skotheim, T. A., Reynolds, J. R., Eds.; CRC Press: Boca Raton, FL, 2006.
(6) Nakano, T.; Okamoto, Y. *Chem. Rev.* **2001**, *101*, 4013.
(7) Ni, S.; Yin, W.; Ferguson-McPherson, M. K.; Satija, S. K.; Morris, J. R.; Esker, A. R. *Langmuir* **2006**, *22*, 5969.
(8) Scherf, U.; List, E. J. W. *Adv. Mater.* **2002**, *14*, 477.
(9) Lieser, G.; Oda, M.; Miteva, T.; Meisel, A.; Nothofer, H.-G.; Scherf, U.; Neher, D. *Macromolecules* **2000**, *33*, 4490.
(10) Knaapila, M.; Stepanyan, R.; Lyons, B. P.; Torkkeli, M.; Monkman, A. P. *Adv. Funct. Mater.* **2006**, *16*, 599.
(11) Knaapila, M.; Lyons, B. P.; Kisko, K.; Foreman, J. P.; Vainio, U.; Mihaylova, M.; Seeck, O. H.; Pålsson, L.-O.; Serimaa, R.; Torkkeli, M.; Monkman, A. P. *J. Phys. Chem. B* **2003**, *107*, 12425.
(12) Tanto, B.; Guha, S.; Martin, C. M.; Scherf, U.; Winokur, M. J. *Macromolecules* **2004**, *37*, 9438.
(13) Chi, C.; Lieser, G.; Enkelmann, V.; Wegner, G. *Macromol. Chem. Phys.* **2005**, *206*, 1597.
(14) Marcon, V.; van der Vegt, N.; Wegner, G.; Raos, G. *J. Phys. Chem. B* **2006**, *110*, 5253.
(15) Knaapila, M.; Stepanyan, R.; Torkkeli, M.; Lyons, B. P.; Ikonen, T. P.; Almásy, L.; Foreman, J. P.; Serimaa, R.; Güntner, R.; Scherf, U.; Monkman, A. P. *Phys. Rev. E* **2005**, *71*, 041802.
(16) Knaapila, M.; Lyons, B. P.; Hase, T. P. A.; Pearson, C.; Petty, M. C.; Bouchenoire, L.; Thompson, P.; Serimaa, R.; Torkkeli, M.; Monkman, A. P. *Adv. Funct. Mater.* **2005**, *15*, 1517.
(17) Grell, M.; Bradley, D. D. C.; Ungar, G.; Hill, J.; Whitehead, K. S. *Macromolecules* **1999**, *32*, 5810.
(18) Chen, S. H.; Chou, H. L.; Su, A. C.; Chen, S. A. *Macromolecules* **2004**, *37*, 6833.
(19) Chunwaschirasiri, W.; Tanto, B.; Huber, D. L.; Winokur, M. J. *Phys. Rev. Lett.* **2005**, *94*, 107402.
(20) Arif, M.; Volz, C.; Guha, S. *Phys. Rev. Lett.* **2006**, *96*, 025503.
(21) Chen, S. H.; Su, A. C.; Su, C. H.; Chen, S. A. *J. Phys. Chem. B* **2006**, *110*, 4007.
(22) Cochran, W.; Crick, F. H. C.; Vand, V. *Acta Crystallogr.* **1952**, *5*, 581.
(23) Petraccone, V.; Pirozzi, B.; Corradini, P. *Eur. Polym. J.* **1972**, *8*, 107.
(24) Hong, S. Y.; Kim, D. Y.; Kim, C. Y.; Hoffmann, R. *Macromolecules* **2001**, *34*, 6474.
(25) Blondin, P.; Bouchard, J.; Beaupré, S.; Belletête, M.; Durocher, G.; Leclerc, M. *Macromolecules* **2000**, *33*, 5874.
(26) Wu, L.; Sato, T.; Tang, H.-Z.; Fujiki, M. *Macromolecules* **2004**, *37*, 6183.
(27) Crick, F. H. C. *Acta Crystallogr.* **1953**, *6*, 689.

MA0626665